Large aperture tunable ultra narrow band Fabry-Perot-Bragg filter

Julien Lumeau[*1], Vadim Smirnov[2], Fabien Lemarchand[3], Michel Lequime[3] and Leonid B. Glebov[1]

[1]School of Optics/CREOL, University of Central Florida, Orlando, FL 32816-2700, USA
[2]OptiGrate 3267 Progress Drive; Orlando, FL, 32826, USA
[3]Institut Fresnel, UMR CNRS 6133, Université Paul Cézanne, 13397 Marseille Cedex 20, France

ABSTRACT

A novel type of filters based on a combination of a Fabry-Perot etalon and a volume Bragg grating is demonstrated. The proposed solid-spaced Fabry-Perot etalon consists of a high quality fused silica window with both faces having identical dielectric mirrors coatings. The transmission of this Fabry-Perot etalon is a discrete channel spectrum consisting of narrow lines (typically a few tens of picometers) which are separated by gaps with constant width defined as the free spectral range (typically between 0.1 and 10 nm). These discrete resonances define the addressable wavelengths. The second element of this complex filter is a volume Bragg grating. This component is obtained by recording of a sinusoidal refractive index modulation into the volume of a photo-thermo-refractive glass plate. Central wavelength of such element can be tuned over several tens of nanometers by rotating the Bragg grating and therefore changing the incidence angle. This element is thus used to select one of the Fabry-Perot resonances and switch between them. We present the features of this filter and two experimental demonstrations of different configurations of Fabry-Perot-Bragg filters combining different Fabry-Perot etalons and volume Bragg gratings. That way, the flexibility of such kind of filters is demonstrated.

Keywords: Volume Bragg grating, Fabry-Perot etalon, narrow band filter, tunable filter

1. INTRODUCTION

Fabry-Perot etalons as narrow-band tunable filters have been widely studied during the past several years. It is well known that the optical thickness of the cavity of a Fabry-Perot filter is directly proportional to its central wavelength. In order to change its optical thickness, the use of piezo-electric and electro-optic [1], or thermo-optic [2] material as a spacer to Fabry-Perot filters has been proposed. However, this did not result in an easy or reliable solution. The two first effects lead only to very low tunability, and the last one means the use of very high temperatures. It has been recently demonstrated that the association of several solid-spaced Fabry-Perot etalons [3] enables the manufacturing of tunable filters with fixed wavelength; however, the design of such filters for a specific application can be complicated, and the rejection band and tunability limited to several tens of nanometers. We propose a new technique consisting of the combination of two optical components: a Fabry-Perot etalon (FPE) and a high-efficiency volume Bragg grating recorded in photo-thermo-refractive (PTR) glass [4, 5]. In this case, the FPE will define a comb of discrete narrow bands (modes) with desirable shape and bandwidth, while the volume Bragg grating which has a high spectral and angular selectivity, will select only one of these modes. The principle of such combination was recently demonstrated with commercial components [6]. In this paper, we present several possible evolutions of this filter in order to improve some of its parameters. We present the use of a high finesse single cavity FPE having ultra-narrow bandpass, and also the use of double cavity FPE having square profile and better rejection. The volume Bragg gratings are either a reflecting Bragg gratings (RBG) and in this case, the diffracted beam is on the same side than the incident beam, or a transmitting Bragg gratings (TBG) and in this case the diffracted beam is on the same side than the transmitted beam. Both types of gratings and their association with FPEs are discussed.

2. NARROWBAND FABRY-PEROT ETALONS

2.1. Ultra-narrowband single cavity Fabry-Perot etalon

The first studied FPE consists of a high quality optical window with both faces having identical coatings. These dielectric mirror coatings are composed of quarter-wave layers alternatively of low (L) and high (H) refractive index. A quarter-wave layer is a layer with optical thickness $n_i t_i$ (n_i being the refractive index of the layer and t_i its thickness) which satisfies the expression: $n_i t_i = \lambda/4$, where λ is the center wavelength of the mirror [7]. Considered materials in our study are silica for L layer (n = 1.44) and tantalum pentoxide for H layers (n = 2.12). These materials are the classical materials used for NIR applications. The transmission of a FPE is a discrete channel spectrum (each resonance has a transmission equal to one assuming no losses) and narrow lines are all separated by gaps with constant width defined as the free spectral range (typically between 0.1 nm and 10 nm). These discrete resonances will define the addressable wavelengths. In this case, the expressions of the spectral width (full width at half maximum ($FWHM_{FPE}$, $\delta\lambda$) and the free spectral range (FSR_{FPE}, $\Delta\lambda$) are [8]:

$$\delta\lambda = \frac{1-R}{\pi\sqrt{R}}\frac{\lambda_0^2}{2n_0 t} \quad and \quad \Delta\lambda = \frac{\lambda_0^2}{2n_0 t} \tag{1}$$

where R is the mirror reflectance, n_0 and t are respectively the refractive index and the thickness of the cavity and λ_0 the central wavelength of the mirrors. For spacer thickness between 100 µm and 5 mm the use of mirrors with a small number of layers (between 3 and 9) is enough to reach a very narrow band-pass (typically several tens or hundreds of picometers). A FPE with the following structure air/H(LH)^4/silica/(HL)^{4}H/air centered at 1064 nm was fabricated. The cavity of the FPE was made with a 0.5 mm thick, 25 mm diameter super-polished and super-parallel fused silica window.

The wedge of this window was characterized with a specific interferometric setup based on interferential spectroscopy [9]. It is less than 1 arcsecond and therefore it is in accordance with the required quality of spacer that permits high transmission of ultra-narrowband FPE [6]. Then, this silica window was coated with identical coatings by Dual Ion Beam Sputtering deposition process. Each 9 layers mirror stack (H(LH)^4) has a reflection coefficient of ~96%. Figure 1 shows the transmission for this FPE. Spectral width of the FPE is 25 pm at FWHM, its FSR is 800 pm and transmission at resonance is higher than 80%. Change of the beam diameter (initial Gaussian beam diameter was ~8 mm and was decreased by insertion of a diaphragm down to 3 mm) did not show major changes in the transmission at the resonances. The evolution of the central wavelength of the final filter was

Figure 1. Experimental and theoretical transmission of the solid-spaced FPE filter for 1064 nm region

also measured. Change of the central wavelength versus beam position is equal to ~ 3 pm/mm and is in accordance with the value of the wedge that was measured previously. Therefore, this preliminary result seems to demonstrate that with such an optical window as spacer, large aperture ultra-narrowband FPE can be obtained. Additional calculations demonstrate that if this FPE is illuminated with a 20 mm aperture collimated Gaussian beam maximum, transmission at the resonance will be higher than 65%. The main losses of FPE, when illuminated with a small beam diameter (fig. 1) are thus resulting from the internal losses in the high refractive index material used in the mirror. Therefore, the improvement of materials properties after coating deposition should permit increasing of transmission of fabricated FPE filters.
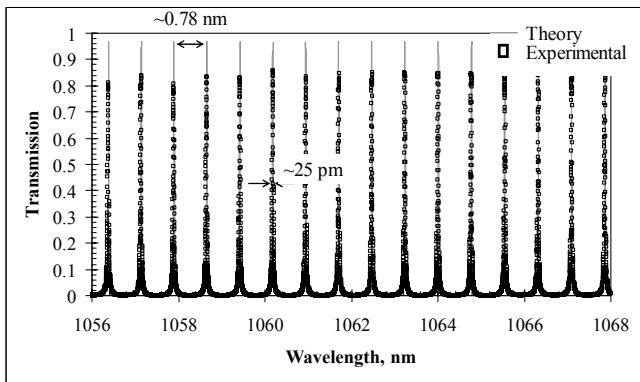
2.2. Narrowband double cavity Fabry-Perot etalon

The second considered FPE was obtained by coherent combination of two identical single cavity FPEs. Central wavelength of the layers is 1555 nm. Each FPE has the following structure: air/H(LH)^3/silica/(HL)^{3}H/air. The cavities were made with a 100 µm thick, 25 mm diameter plane parallel fused silica window. Wedges were also measured and are equal to ~3 arcseconds and both cavities have exactly the same thickness. Then, these silica windows were coated with identical coatings by Ion Beam Sputtering deposition process. These coatings are 7-layers mirrors with the

following structure: H(LH)[3] centered at 1555 nm. H and L are quarter-wave layers at central wavelength with respectively a high (Ta2O5) and a low refractive (SiO2) indices. Therefore, the FWHM of each single cavity is about one order of magnitude larger than the FWHM of the FPE described above. In order to obtain a coherent combination of the two FPEs, an additional 0.5L layer was deposited on one side of each cavity above the dielectric mirror. Then adhesion process was performed between these 2 layers in order to create a L coupling layer. A comprehensive description of the features of such filter is given in ref. [10] and additional information regarding contacting process and FPE characterization is given in ref. [11]. The transmission of the resulting double cavity FPE is shown in figure 2. One can see that the filter shows a comb of narrowband filters, with spectral width

Figure 2. Experimental and theoretical transmission of the double cavity FPE filter for 1550 nm region

of ~0.6 nm at FWHM and equally separated by the FSR equal to ~8 nm. Moreover, each resonance has a square profile, and maximum at resonance contains oscillations. As discussed in the ref. [10], these resonances are linked to the filter's design and can be decreased and even canceled by changing the design of the mirror. One solution consists for example in changing the optical thickness of the last layer of the external mirrors.
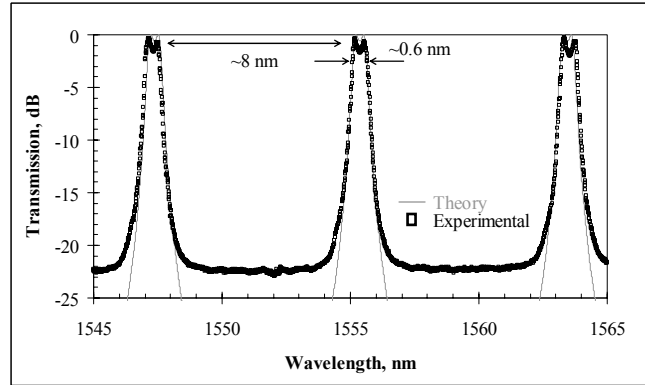
3.   VOLUME BRAGG GRATINGS

3.1.   Reflecting volume Bragg grating

The first volume Bragg grating which was studied is a reflecting Bragg grating (RBG). This component is obtained by recording of a sinusoidal refractive index modulation in a photosensitive medium. With such RBG, plane of iso-refractive indices are parallel to the faces of the window in which it was recorded and beam is diffracted in the same side than the reflected one. A RBG is a narrow-band reflection filter. Typical bandwidth is equal to less than 1 nm and angular selectivity is generally between 1 and 100 mrad. The key point of this filter is that the central wavelength of the RBG can be tuned by rotating the Bragg grating and therefore changing the incidence angle on the grating [12]:

$$\lambda_0 = \cos\left(\text{asin}\left(\frac{\sin(\theta)}{n_{PTR}} \right) \right) \cdot \lambda_R \qquad (2)$$

where θ is the angle of incidence, and λ_0 the resonant Bragg wavelength. A RBG was fabricated by holographic recording at OptiGrate Company inside photo-thermo-refractive (PTR) glass. PTR glass is a multi-component silicate

glass which possesses photosensitive properties. When exposed to UV-radiation and then thermally developed, refractive index as high as 1000 ppm can be induced in this glass. Finally, high efficiency holographic elements were previously demonstrated in this glass [4].

The first grating was designed such as its central wavelength (λ_R) is equal to 1065.5 nm. Hence grating period (Λ) is fixed and equal to $\Lambda = \lambda_R 2n_0$, where n_0 is the refractive index of the photosensitive medium. For low inclination of the grating, the evolution of the spectral dependence of the diffraction efficiency (DE) was measured (Fig. 3). In this case central wavelength is equal to ~1060 nm. Moreover this RBG has a spectral selectivity of ~450 pm (FWHM) and a diffraction efficiency of ~99%. One can see that oscillations appear
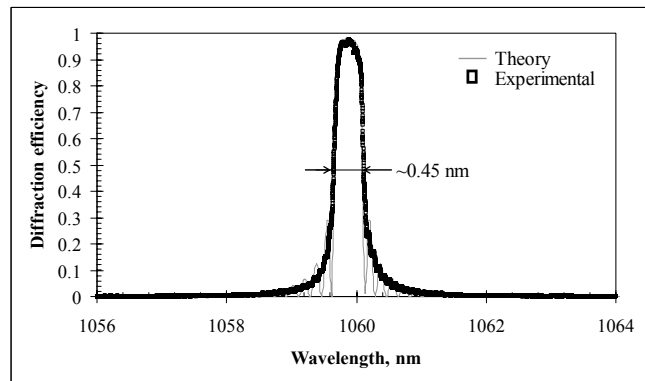
Figure 3. Diffraction efficiency of the RBG for 1064 nm region

around the main lobe of the reflection. These oscillations are typical for uniform Bragg gratings [12]. However, these side lobes can be eliminated by the use of gratings with special variations of the magnitude of the refractive index modulation, so called apodized gratings [13].

3.2. Transmitting volume Bragg grating

The second diffractive element that was used in our demonstration is a transmitting Bragg grating (TBG). Detailed description of the theory of TBGs is given in ref [14]. This component is obtained by recording of a sinusoidal refractive index modulation in a photosensitive medium. With such a grating, planes of iso-refractive indices are perpendicular to the faces of the window and diffracted beam exits the TBG through the back side of grating. TBG are generally very good angular filters (angular selectivity between 0.05 and 25 mrad) and have typical spectral selectivity between 0.5 and 40 nm.
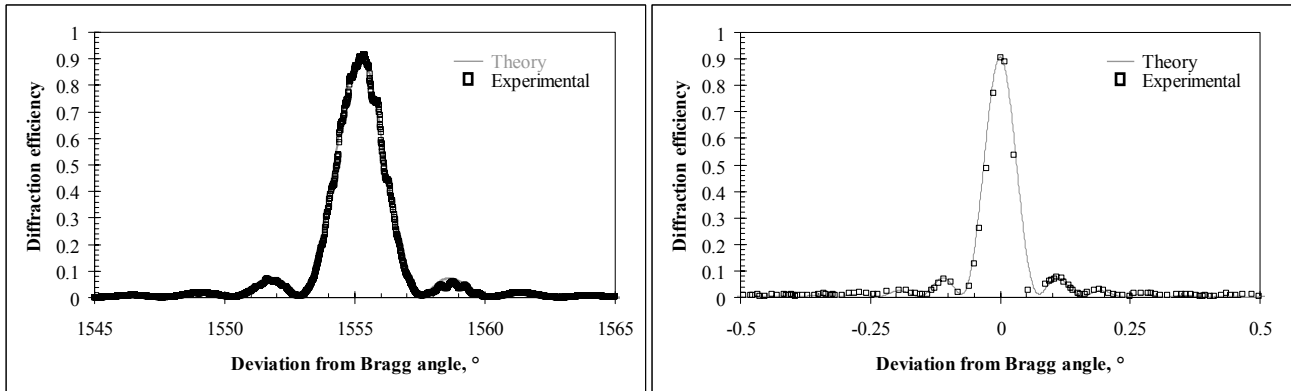

Figure 4. Diffraction efficiency versus wavelength (left graph) and deviation from Bragg angle (right graph) measured on the transmitting Bragg grating for 1550 nm region

The TBG that we considered has the following parameters: 1.52 mm thickness, grating period Λ is equal to 1.12 µm. Such a TBG was fabricated by holographic recording at OptiGrate Company inside photo-thermo-refractive glass. Evolution of the diffraction versus wavelength and deviation from Bragg angle were measured and are plotted in figure 4. Spectral selectivity of the fabricated TBG is ~2 nm (FWHM), its angular selectivity (acceptance angle) is ~0.9 mrad and its diffraction efficiency is higher than 90%. It is seen that this TBG will be at the same time a good spectral and angular filter. This remark implies the usage of collimated beam with diameter larger than 5 mm for its characterization in order to obtain high diffraction efficiency and resolve it angular and spectral shape.

4. FABRY-PEROT-BRAGG FILTERS

The characterization of ultra-narrow band filters requires high spectral resolution of test equipment. Thus, narrow band tunable lasers have been used for high resolution measurements. One laser had a tuning range 1050-1070 nm (New Focus Velocity 6000). The spectral line width of this laser is less than 1 pm with fine tuning step ~1 pm. The set up for measurements of spectral selectivity of RBGs, FPE and FPB by means of these lasers is shown in figure 5. Light emitted by the single mode laser is collimated by a telescope. Beam diameter was equal to ~8 mm. Moreover, in order to change beam diameter, an iris diaphragm is placed immediately after the collimator. This collimated beam is send through the FPE and is reflected by the RBG. In order to carry out fine tuning of the RBG, this last is mounted on motorized computer controlled rotation stages. Finally, a silicon detector is placed in front of the diffracted beam in order
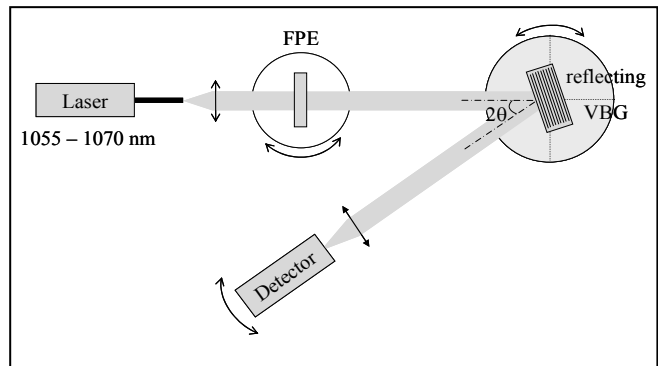

Figure 5. Basic setup used for the characterization of the assembled reflecting FPB filters for 1064 nm region

to measure the throughput of the filter. This detector is finally associated with data acquisition and all the measurement is computer controlled with Labview programs. An identical setup was used for the characterization of the filters at 1550 nm. A Santec TLS200 laser that can continuously change its output wavelength from 1530 to 1590 nm with a 1 pm step was used in this setup. The detector used for the power measurements is a Thorlabs InGaAs amplified detector. Configuration of the setup is identical to the configuration that is used at 1060 nm and depicted in Fig. 6. Main differences with the setup at 1064 nm is that the diameter of the beam exiting the collimator is ~6 mm and that the
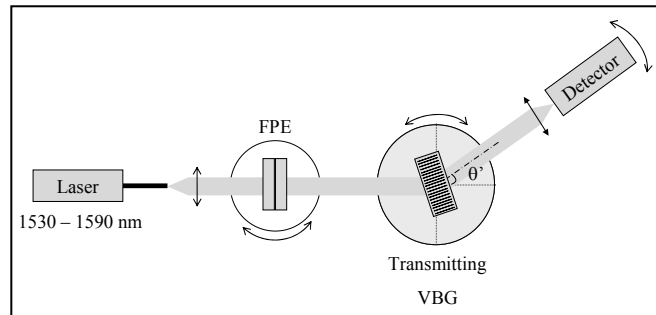

Figure 6. Basic setup used for the characterization of the assembled transmitting FPB filters for 1550 nm region

detector measuring diffracted beam is positioned on the same side than the transmitted beam.

4.1. Reflecting 25 pm bandwidth filter for 1060 nm region

The 25 pm bandwidth single cavity FPE and the RBG were combined in order to obtain a reflecting ultra-narrowband Fabry-Perot-Bragg (FPB) filter (figure 5). Throughput of the filter was measured for low inclination of the grating. In this case the filter is centered at 1064.9 nm. The spectral selectivity of the proposed narrow band filter resulting from the incoherent association of this RBG and the FPE is presented in Fig.7. Only one resonance appears in a wide spectrum. And this unique narrow band resonance has a 25 pm bandwidth at FWHM. It can be seen that two small resonances (T < 1%) are still visible close to the main resonance peak. We investigated in details the origin of these peaks. To succeed, we changed the inclination of our filter in order to obtain a new coincidence between the FPE and the RBG at a different wavelength (~1055 nm). Then

Figure 7. Throughput of the FPB filter for 1064 nm region, for low inclination of the RBG

diffraction efficiency of the RBG and throughput of the FPB filter were recorded for the same RBG inclination.

Measurements are represented in Fig. 8. This graph demonstrates that rejection of the RBG is very efficient only about 6 nm away from the resonant wavelength. Outside this band, rejection is higher than 30 dB (detection limit of our measurement setup). Inside this 6-nm band, rejection is better than 30 dB except for 25 pm width narrow lines, equally separated by 0.8 nm and coinciding with the FPE resonances. At these resonant wavelengths, rejection is however better than 20 dB. A way to improve this rejection close to the main peak would first consist in manufacturing a new RBG with narrower line (such as 0.2 nm). Moreover, apodization of this grating would also permit to improve rejection. Finally, according the very low level of losses of the RBG, rejection improvement could consist in associating at least 2 parallel RBG. Such solution would also have as consequence to avoid any rotation of the output beam when the RBG is rotated.
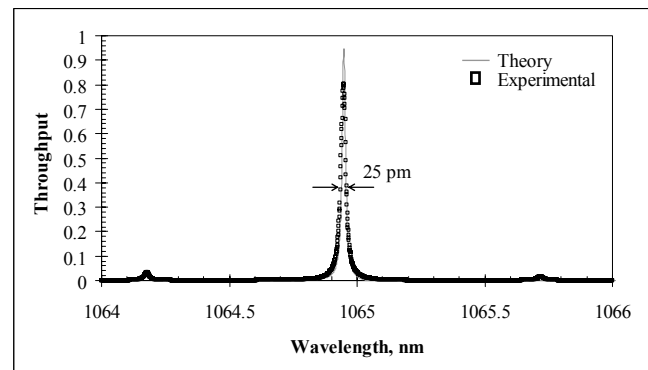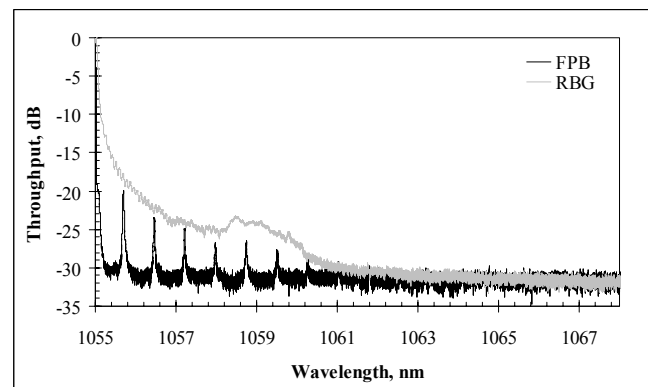

Figure 8. Throughput of the FPB filter for 1064 nm region, for larger inclination of the RBG: in black, the throughput of the FPB filter and in gray the diffraction efficiency of the RBG

As it was introduced in the sections 2, the designed and manufactured FPB filters can be tuned by several tens of nanometers. RBG was originally centered at 1065.5 nm. However, the central wavelength of the RBG can be tuned to lower wavelengths by rotating it. Therefore, it is possible to select any resonant wavelength of the FPE by changing the inclination (rotating) of the RBG. Moreover, since the spectral response of the final filter is determined by the FPE, no distortion of this spectral response will appear during tuning. Therefore we tilted the filter with three different angles (~2.8°, ~7.9°, ~11.2°) and measured the spectral dependence of the throughput of the FPB filter. Figure 9 demonstrates the tunability of this filter over 10 nm without any spectral shape distortion and constant bandwidth equal to 25 pm. Moreover, it is important to emphasize that only discrete tunability of our filter was investigated. Continuous and fine tunability can

Figure 9. Throughput of the FPB filter for 1064 nm region, for different inclination (α) of the RBG: curve 1: α ~ 2.8°, curve 2: α ~ 7.9°, curve 3: α ~ 11.2°

be obtained if the inclination of the FPE is also adjusted to the desirable wavelength. According to the free spectral range of FPE which is be limited to several tenths of nanometer, inclinations of the FPE of a few degrees would be enough to shift the whole comb by one free spectral range and therefore tune to all the addressable wavelengths.
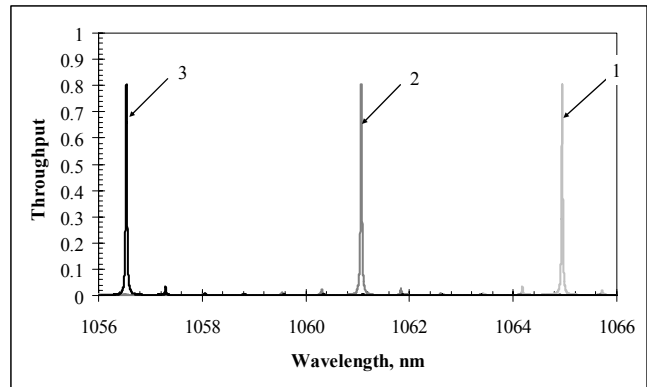
4.2. Transmitting double cavity filter for 1550 nm region

The second configuration consists in the combination of the double cavity FPE and the TBG (figure 6). Throughput of the filter was measured for one inclination of the TBG corresponding to a coincidence with a resonance of the FPE (figure 10). One can see that TBG has larger spectral selectivity than the RBG. Hence this justifies the use of FPE with large FSR, in order to allow the TBG to select only one resonance of the FPE. Therefore the filter presents only one resonance which shape is given by the FPE and throughput higher than 80%. Outside the resonance, the rejection is given by the product if the diffraction efficiency of the TBG and the transmission of the FPE. All remarks regarding improvement of the rejection (apodization, combining of two RBGs or TBGs) can be applied to this configuration too.
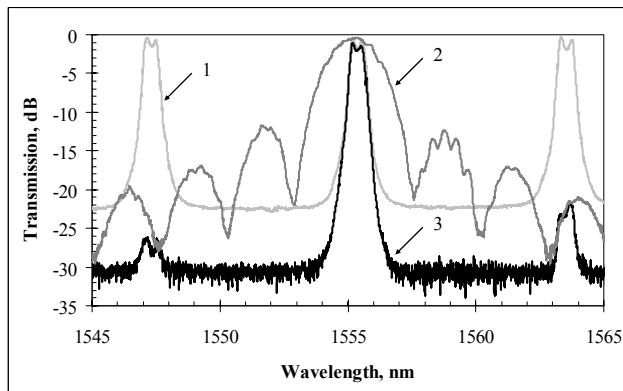
Figure 10. Throughput of the double cavity FPE (curve 1), of the TBG (curve 2) and of the FPB filter (curve 3) for one inclination of the transmitting TBG
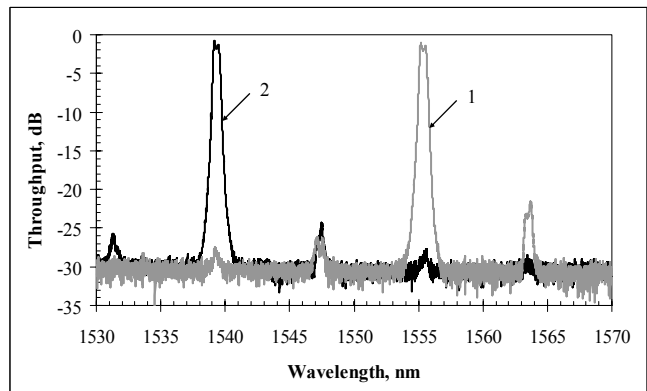
Figure 11. Throughput of the FPB filter for 1550 nm region, for 2 different inclination of the TBG (curves 1 and 2)

Moreover, it is important to note that the FPB filter will have high spectral selectivity of a few hundreds of picometers (even tens of picometers if mirrors with higher reflection coefficients are used) due to the use of FPE and also high angular selectivity of 0.8 mrad due to the use of TBG. In this manner, best of each element can be captured and combined into one unique filter. Finally, the filter was tuned by 15 nm after changing the inclination of the TBG. Spectral dependence of the throughput of the filter was measured and is shown in figure 11.

5. CONCLUSION

A tunable narrowband filter combining a volume Bragg grating and a Fabry-Perot etalon is proposed. The combination of a high finesse Fabry-Perot with 25 pm bandwidth and a reflecting Bragg grating is first experimentally demonstrated. Prototype shows very good agreement with theory and a throughput higher than 80%. Then an alternative combination of a double cavity FPE and a TBG is investigated. Fabricated filter also shows very good optical properties and large tunability. By this way, flexibility and performances of Fabry-Perot-Bragg filter is demonstrated.

6. ACKNOWLEDGEMENTS

7. REFERENCES

[1] M. Lequime, R. Parmentier, F. Lemarchand and C. Amra "Toward tunable thin-film filters for wavelength division multiplexing applications", *Appl. Opt*. 41, 3277-3284 (2002).

[2] L. Domash*,* M. Wu, N. Nemchuk, and E. Ma, "Tunable and switchable multiple-cavity thin film filters", *Journal of Lightwave Technology* 22 (1), 126-135 (2004).

[3] J. Floriot, F. Lemarchand and M. Lequime, "Tunable double-cavity solid-spaced Bandpass filter", *Optics Express* 12 (25), 6289-6298 (2004).

[4] O. M. Efimov, L. B. Glebov, L. N. Glebova, K. C. Richardson and V. I. Smirnov, "High-efficiency Bragg gratings in photo-thermo-refractive glass", *Appl. Opt.* 38, 619–627 (1999).

[5] O.M. Efimov, L.B. Glebov, L.N. Glebova and V.I. Smirnov, "Process for production of high efficiency volume diffractive elements in photo-thermo-refractive glass", United States Patent 6,586,141 B1. (2003).

[6] J. Lumeau, V. Smirnov and L.B. Glebov, "Tunable narrow-band filter based on a combination of Fabry-Perot etalon and Volume Bragg Grating", *Optics Letters* 31 (16), 2417-2419 (2006).

[7] M. Born and E.Wolf, "Principles of Optics", 7th edition, Cambridge University Press (1999).

[8] H. Kogelnik, "Coupled wave theory for thick hologram gratings", *Bell Syst. Tech. J.* 48, 2909-2947 (1969).

[9] J. Lumeau and M. Lequime, "Localized measurement of the optical thickness of a transparent window - Application to the study of the photosensitivity of organic polymers", *Applied Optics* 45 (4), 6099 – 6105 (2006).

[10] J. Floriot, F. Lemarchand, and M. Lequime "Solid-spaced filters: an alternative for narrow-bandpass applications" *Appl. Opt.* 45 (7), 1349-1355 (2006).

[11] J. Floriot, F. Lemarchand, L. Abel-Tiberini and M. Lequime, "High accuracy measurement of the residual air gap thickness of thin-film and solid-spaced filters assembled by optical contacting", *Optics Communications* 260 (1), 324-328 (2006).

[12] J.M. Tsui, C. Thompson, V. Mehta, Jeffrey M. Roth, V.I. Smirnov and L.B. Glebov, "Coupled-wave analysis of apodized volume gratings", *Opt. Express* 12, 6642-6653 (2004).

[13] E. Rotari, L. Glebova and L. B. Glebov, "Refractive index modulation in photo-thermo-refractive fibers", *Proc. of SPIE* 5709, 379–384 (2005).

[14] I.Ciapurin, L.Glebov, and V.Smirnov. "Modeling of phase volume diffractive gratings, part 1: Transmitting sinusoidal uniform gratings", *Optical Engineering* 45 015802 (2006).